Monthly Notices
of the
ROYAL ASTRONOMICAL SOCIETY

Mon. Not. R. Astron. Soc. **421,** 2478–2484 (2012) doi:10.1111/j.1365-2966.2012.20478.x

Population gradients in the Sloan Digital Sky Survey Galaxy Catalogue: the role of merging

C. Tortora[1]★ and N. R. Napolitano[2]

[1] *Universität Zürich, Institut für Theoretische Physik, Winterthurerstrasse 190, CH-8057 Zürich, Switzerland*
[2] *INAF – Osservatorio Astronomico di Capodimonte, Salita Moiariello, 16, 80131 Napoli, Italy*

Accepted 2012 January 2. Received 2011 December 9; in original form 2011 October 7

ABSTRACT

We investigate the role of the environment on the colour and stellar population gradients in a local sample of ∼3500 central and ∼1150 satellite Sloan Digital Sky Survey (SDSS) early-type galaxies. The environment is parametrized in terms of the number of satellite galaxies, $N_{\rm gal}$, in each group. For central galaxies, we find that both optical colour and mass-to-light (M/L) ratio gradients are shallower in central galaxies residing in denser environments (higher $N_{\rm gal}$). This trend is driven by metallicity gradients, while age gradients appear to be less dependent on the environment and to have a larger scatter. On the other hand, satellites do not show any differences in terms of the environment. The same results are found if galaxies are classified by central age, and both central and satellite galaxies have shallower gradients if they are older and steeper gradients if younger, satellites being independent of ages. In central galaxies, we show that the observed trends can be explained with the occurrence of dry mergings, which are more numerous in denser environments and producing shallower colour gradients because of more uniform metallicity distributions due to the mixing of stellar populations, while no final clues about merging occurrence can be obtained for satellites. Finally, we discuss all systematics on stellar population fitting and their impact on the final results.

Key words: galaxies: elliptical and lenticular, cD – galaxies: evolution – galaxies: general.

1 INTRODUCTION

Colour and stellar population gradients in galaxies are providing important clues to galaxy evolution (Hopkins et al. 2009; Spolaor et al. 2009, 2010; Kuntschner et al. 2010; Pipino et al. 2010; Rawle, Smith & Lucey 2010; La Barbera et al. 2011; Tortora et al. 2010, 2011a; Tortora et al. 2011b, hereafter T+11). The value of metallicity and age gradients and their trends with the mass have been recently investigated on samples of local early-type galaxies (ETGs), suggesting that different physical phenomena could concur to shape the gradients at low and high masses (e.g. Tortora et al. 2010, hereafter T+10). From one side, gas infall and supernovae feedback (Larson 1974, 1975; Kawata 2001; Kawata & Gibson 2003; Kobayashi 2004; Pipino et al. 2010; Tortora et al. 2011a) seem to be the main phenomena driving the evolution of low-mass ETGs, while merging and active galactic nucleus feedback (Kobayashi 2004; Sijacki et al. 2007; Hopkins et al. 2009) would work at larger masses (Dekel & Birnboim 2006). However, environment also plays a crucial role in galaxy evolution, since many physical phenomena like tidal interactions, strangulations and harassment would affect the star formation in low-mass galaxies (e.g. Weinmann et al. 2009) and cause inner population gradients at different mass scales (e.g. Tortora et al. 2011a). In more massive systems, though, the major player in driving the stellar population mixing is galaxy merging (Davis et al. 1985; Springel et al. 2005; Romeo et al. 2008). Kobayashi (2004) has shown that overall merging events tend to flatten the metallicity gradients with time. Looking in more details, merging events can have a complex taxonomy; thus, minor or major merging, or even gas-rich or gas-poor merging are expected to produce different stellar population gradients. For instance, after the initial gas-rich merging events (generally occurring at high redshift), larger central metallicity and positive age gradients are observed (Mihos & Hernquist 1994; Kobayashi 2004); subsequent gas-poor merging may dilute the positive age gradient with time as well as make the metallicity gradients flattened out (White 1980; Di Matteo et al. 2009; Hopkins et al. 2009).

Although higher mass systems would be the ones which have experienced a larger fraction of merging events, it is also interesting to investigate if central galaxies in groups and clusters may differ, in their population gradient properties, from satellite systems orbiting in the cluster potential. The central galaxies in clusters (and groups) are the most luminous and massive (in terms of stellar mass) objects in the Universe. They are found to have different luminosity profiles when compared with typical cluster galaxies (Schombert 1986) and do not seem to be drawn from the same luminosity function as bright

★E-mail: ctortora@physik.uzh.ch

ellipticals (Dressler 1978; Bernstein & Bhavsar 2001). These evidences suggest that the evolutive processes of central galaxies can be strongly different from the ones driving normal (satellite) systems. Moreover, they still hold imprints from the early evolutionary stages since they reside in the very central regions of clusters and groups, where mass started to be accreted earlier after the big bang than other density environments. During the cosmic time, these regions have witnessed a variety of galaxy interactions with the environment and merging events (e.g. Romeo et al. 2008) which have contributed to the mass accretion of larger and larger galaxy systems, a process which is more efficient in denser environments like group/cluster haloes (e.g. Stott et al. 2008, 2010; Whiley et al. 2008).

From this perspective it is natural to expect that the galaxy in the centre of very dense environments might be more sensitive to the effect of the large amount of merging events expected in the hierarchical growth which shall be recorded in the stellar population parameters (e.g. age and metallicity).

Thus, we have considered a local sample of Sloan Digital Sky Survey (SDSS) galaxies (Blanton et al. 2005), recently analysed and discussed in T+10 and T+11, where we have discussed colour, mass-to-light ratio (M/L) and stellar population gradients in terms of mass and compared with independent observations. These results have been framed within the predictions of hydrodynamical and chemodynamical simulations of galaxy formation. In this paper we will discuss the connection with the environment, selecting those galaxies classified as centrals and satellites in groups and clusters and investigating if gradients change as a function of the environment.

The paper is organized as follows. The data sample and the analysis have been presented in Section 2, the results are discussed in Section 3, while Section 4 is devoted to the physical interpretation and conclusions. Systematics in stellar population fit have been discussed in Appendix A.

2 DATA AND SPECTRAL ANALYSIS

We start from a data base consisting of 50 000 low-redshift ($0.0033 \leq z \leq 0.05$) galaxies in the New York University Value-Added Galaxy Catalogue (NYU-VAGC) extracted from SDSS DR4 (Blanton et al. 2005, hereafter B05),[1] recently analysed in T+10 and T+11,[2] where stellar population synthesis models have been used to determine galaxy stellar mass, M_*, colour and stellar population parameters/gradients. Following T+10, we have sorted out ETGs by keeping those systems with a Sérsic index satisfying the condition $2.5 \leq n \leq 5.5$ and with a concentration index $C > 2.6$. The final ETG sample consists of 10 508 galaxies. We have cross-matched our data sample with the ($z > 0.01$) DR4 SDSS based group catalogue from Yang et al. (2007) to recover information about the environment the galaxies live. Yang et al. (2007) have identified the groups and have separated the most massive (or most luminous) galaxies in each group, labelled as centrals, from the satellites. We will use both (1) the identification of satellites and centrals on the basis of stellar mass selection and (2) the number of galaxies $N_{\rm gal}$ in each group as an environment indicator. We have retained galaxies – isolated (having $N_{\rm gal} = 1$), central and satellite – with a mass $\log M_*/{\rm M}_\odot > 10.5$ and left with a final sample of 3525 central (including 1941 isolated systems) and 1141 satellite galaxies. As a further criterion, we have also ranked satellites in each group on the basis of their stellar masses.

We note that the fraction of central ETGs in each mass bin is lower than the fraction of satellite and field galaxies at $\log M_*/{\rm M}_\odot \lesssim 10.7-10.9$, while it increases at larger masses, with 62 centrals, 6 satellites and 1 field galaxy for $\log M_*/{\rm M}_\odot > 11.4$.

As discussed in T+10, we have used structural parameters given by B05 to derive the colour profile $(X - Y)(R)$ of each galaxy as the differences between the (logarithmic) surface brightness measurements in the two bands, X and Y. The stellar population properties are derived by the fitting of Bruzual & Charlot (2003, hereafter BC03) 'single burst' synthetic stellar models to the observed colours. Age and metallicity are free to vary, and a Chabrier (2001) initial mass function is assumed. However, in order to check the effect of the existing degeneracies between age and metallicity, we will also assume the age gradient to zero (T+11) by fixing the age to 10 Gyr as a prior.[3] We define the CG as the angular coefficient of the relation $X - Y$ versus $\log R/R_{\rm eff}$, $\nabla_{X-Y} = \frac{\delta(X-Y)}{\delta \log(R/R_{\rm eff})}$, measured in mag dex^{-1} (omitted in the following), where $R_{\rm eff}$ is the r-band effective radius. By definition, a positive CG, $\nabla_{X-Y} > 0$, means that a galaxy is redder as R increases, while it is bluer outwards for a negative gradient. The fit of synthetic colours is performed on the colours at $R_1 = R_{\rm eff}/10$ and $R_2 = R_{\rm eff}$ and on the total integrated colours. Stellar parameter gradients are defined as $\nabla_W = \frac{\delta \log(W)}{\delta \log(R/R_{\rm eff})}$, where $W = ({\rm age}, Z, \Upsilon_*)$ are the estimated age, metallicity and M/L. Because of the definitions adopted for R_1 and R_2, an easier and equivalent definition can be used; in fact, we define $\nabla_{\rm age} = \log[{\rm age}_2/{\rm age}_1]$, $\nabla_Z = \log[Z_2/Z_1]$ and $\nabla_{\Upsilon_*} = \log[\Upsilon_{*2}/\Upsilon_{*1}]$, where $({\rm age}_i, Z_i, \Upsilon_{*i})$, with $i = 1, 2$, are the estimated parameters at R_1 and R_2, respectively.

In T+10 and T+11, we have discussed the impact of the wavelength coverage on the results. Here, we will add further Monte Carlo simulations in order to verify that the optical bands alone introduce small spurious degeneracies and/or correlations among parameters with respect to stellar models including near-IR or UV data. In particular, we will quantify any systematics and possible trends with stellar mass and $N_{\rm gal}$ in Fig. A1, and discuss the impact on our results in Section 4.

3 GRADIENTS AND ENVIRONMENT

In T+10 and T+11 we have discussed the colour, age, Z and M/L gradients as a function of stellar mass without distinguishing central from satellite galaxies. Here, we will expand the analysis by investigating the effect of the environment on the most massive central and satellite galaxies, showing the significance of the correlations in Table 1 and the slopes in Table 2.

We start in Fig. 1 by showing the gradients ∇_{g-r}, ∇_{Υ_*}, ∇_Z and $\nabla_{\rm age}$ as a function of the stellar mass for central and satellite galaxies. The trend of central galaxies alone does not differ much from the one of the total sample studied in T+10 and T+11. They have colour and metallicity gradients which become shallower at larger masses. ∇_{Υ_*} values are negative at low masses, turn out to be null around $\log M_*/{\rm M}_\odot \sim 11$ and finally become slightly positive at very high masses. The positive trend of $\nabla_{\rm age}$ is statistically significant (as shown in Tables 1 and 2) despite its large scatter. ∇_Z show

[1] The catalogue is available at http://sdss.physics.nyu.edu/vagc/lowz.html.

[2] Details about sample selection, incompleteness and biases can be found in T+10.

[3] As we will also discuss later, $\nabla_{\rm age} = 0$ is a reasonable assumption for the older galaxies, which are found to have $\nabla_{\rm age} \sim 0$ (Tortora et al. 2010).

Table 1. Sign of the correlation between gradients and M_* or $N_{\rm gal}$ and confidence limits (given in per cent). The significance of the correlation is obtained by applying the Student's t-distribution to the Spearman rank factor.

	Centrals		Satellites	
$\nabla_{\rm g-r}$–M_*	↑ (99)		↑ (95)	
∇_{g-r}–$N_{\rm gal}$	↑ (99)		↑ (95)	
	All free	$\nabla_{\rm age}=0$	All free	$\nabla_{\rm age}=0$
$\nabla_{\rm age}$–M_*	↑ (99)	–	↑ (99)	–
∇_Z–M_*	↑ (95)	↑ (99)	Null (99)	↑ (99)
∇_{Υ_*}–M_*	↑ (99)	↑ (99)	↑ (99)	↑ (99)
$\nabla_{\rm age}$–$N_{\rm gal}$	↑ (90)	–	Null (99)	–
∇_Z–$N_{\rm gal}$	↑ (99)	↑ (99)	↑ (95)	↑ (99)
∇_{Υ_*}–$N_{\rm gal}$	↑ (99)	↑ (99)	↑ (95)	↑ (95)

Table 2. Slopes of the correlation between gradients and M_* or $N_{\rm gal}$ and 1σ uncertainties derived by bootstrap method.

	Centrals		Satellites	
$\nabla_{\rm g-r}$–M_*	0.06 ± 0.01		0.04 ± 0.02	
∇_{g-r}–$N_{\rm gal}$	0.03 ± 0.01		0.01 ± 0.01	
	All free	$\nabla_{\rm age}=0$	All free	$\nabla_{\rm age}=0$
$\nabla_{\rm age}$–M_*	0.21 ± 0.04	–	0.28 ± 0.07	–
∇_Z–M_*	0.23 ± 0.04	0.30 ± 0.04	0.17 ± 0.09	0.26 ± 0.05
∇_{Υ_*}–M_*	0.20 ± 0.02	0.12 ± 0.01	0.26 ± 0.06	0.10 ± 0.02
$\nabla_{\rm age}$–$N_{\rm gal}$	0.08 ± 0.04	–	0.02 ± 0.04	–
∇_Z–$N_{\rm gal}$	0.12 ± 0.02	0.13 ± 0.03	0.05 ± 0.04	0.05 ± 0.02
∇_{Υ_*}–$N_{\rm gal}$	0.11 ± 0.02	0.05 ± 0.01	0 ± 0.02	0.01 ± 0.01

an increasing trend with M_* (from -0.5 to -0.3 across the mass range), although the scatter at lower masses is quite large.

If one forces $\nabla_{\rm age}=0$ (assuming ${\rm age}_1={\rm age}_2=10\,{\rm Gyr}$), ∇_Z values are rigidly shifted towards larger values and show a steeper trend with stellar mass, with $\nabla_Z\sim0$ for the most massive galaxies. Similarly, ∇_{Υ_*} are shifted towards more negative values while their trend with mass is shallower (see T+11). Note that in case of no age gradients, (negative) shallower ∇_{Υ_*} values naturally correspond to (negative) shallower colour and metallicity gradients. In contrast, in presence of non-zero age gradients negative colour gradients could correspond to positive M/L gradients due to recent star formation episodes. Almost all of these correlations are significant at more than 99 per cent (see Table 1).

Satellite galaxies behave differently from centrals. Colour gradients are less dependent on mass, while the ∇_{Υ_*} trend is steeper with mass. This is driven by the $\nabla_{\rm age}$ which is increasing at the higher mass bins, being ∇_Z less dependent on M_*. The fact that the ∇_{Υ_*} trend is mainly driven by the age gradients is confirmed when forcing $\nabla_{\rm age}=0$; in this case the trend of ∇_{Υ_*} with mass gets shallower although ∇_Z show a steep increasing trend with M_*.

In Fig. 2, colour, metallicity, age and M/L gradients are plotted as a function of $N_{\rm gal}$. We find that in denser environments (higher $N_{\rm gal}$) central galaxies have shallower colour gradients, going from $\nabla_{\rm g-r}\sim-0.09$ in the field to $\nabla_{\rm g-r}\sim-0.04$ in the clusters ($N_{\rm gal}\gtrsim50$). This trend is reproduced by a similar behaviour of metallicity gradients which are on average ~-0.5 in the field and ~-0.3 in denser environments. On the contrary, $\nabla_{\rm age}$ are only slightly steeper in densest environments. According to the trends of colour and Z gradients, ∇_{Υ_*} tend to be steeper in the field (~-0.05), almost null in poor groups ($N_{\rm gal}\sim10$), while they are positive (~0.1) at $N_{\rm gal}\gtrsim50$. The trends with environment are clearer if we divide the sample in terms of the central age, ${\rm age}_1$. Three age intervals are adopted, i.e. $0<{\rm age}_1\leq6$, $6<{\rm age}_1\leq10$ and ${\rm age}_1>10$, which gather 1808, 594, 1123 centrals and 577, 198, 366 satellites, respectively. Older galaxies have progressively shallower age and metallicity gradients, independently from $N_{\rm gal}$ (see also the discussion in T+10). The trends with $N_{\rm gal}$ are still statistically significant for ∇_Z, which become shallower going from the field to denser environments by ~0.15, 0.2, 0.4, while the correlations for $\nabla_{\rm age}$ get flat for each age bin. The behaviour of ∇_{Υ_*} is different: oldest galaxies have negative ∇_{Υ_*} (~-0.2, -0.1) with a shallower trend with $N_{\rm gal}$ (in the very rich systems they are almost zero), while the youngest ones have positive gradients (~0.05, 0.15), which get larger in higher density environment.

On the contrary, satellite galaxies have gradients which are completely independent of the environment they live (see slopes in Table 2). To have a complete view of behaviours in satellites, we have also considered the rank-2 satellites, i.e. the second most massive galaxy in each group, and plotted their gradients in the right-hand panel of Fig. 2. Here, we see little changes in the ∇_{g-r} and ∇_Z trends, while $\nabla_{\rm age}$ and ∇_{Υ_*} seem to be steeper functions of $N_{\rm gal}$, with steeper values in very high density environment. To avoid a too low statistics, we have not investigated higher rank systems.

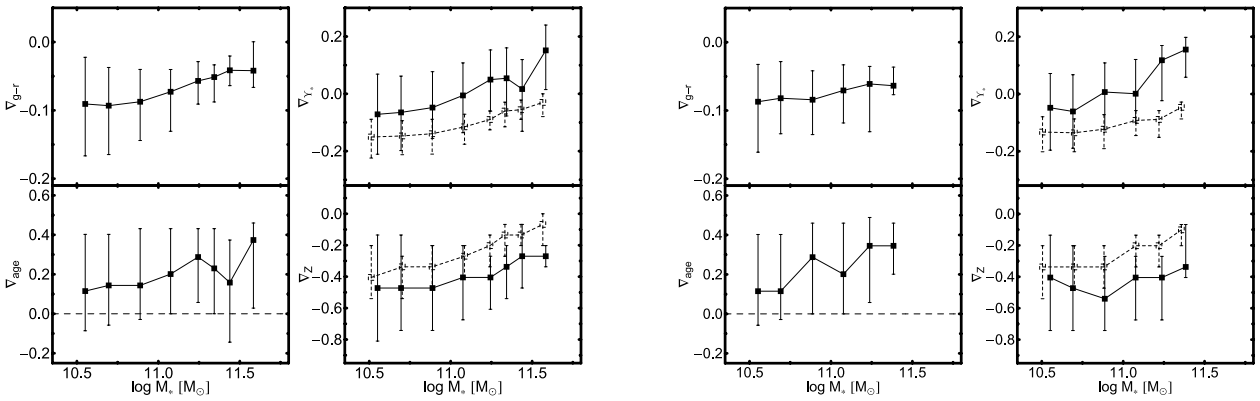

Figure 1. Gradients in terms of stellar mass for centrals (left) and satellites (right). In each panel, we show $g-r$ (top left), M/L (top right), age (bottom left) and Z (bottom right) gradients as a function of stellar mass. The medians and 25–75th quantiles are shown. The dashed symbols are for the case with $\nabla_{\rm age}=0$ (i.e. ${\rm age}_1={\rm age}_2=10\,{\rm Gyr}$).

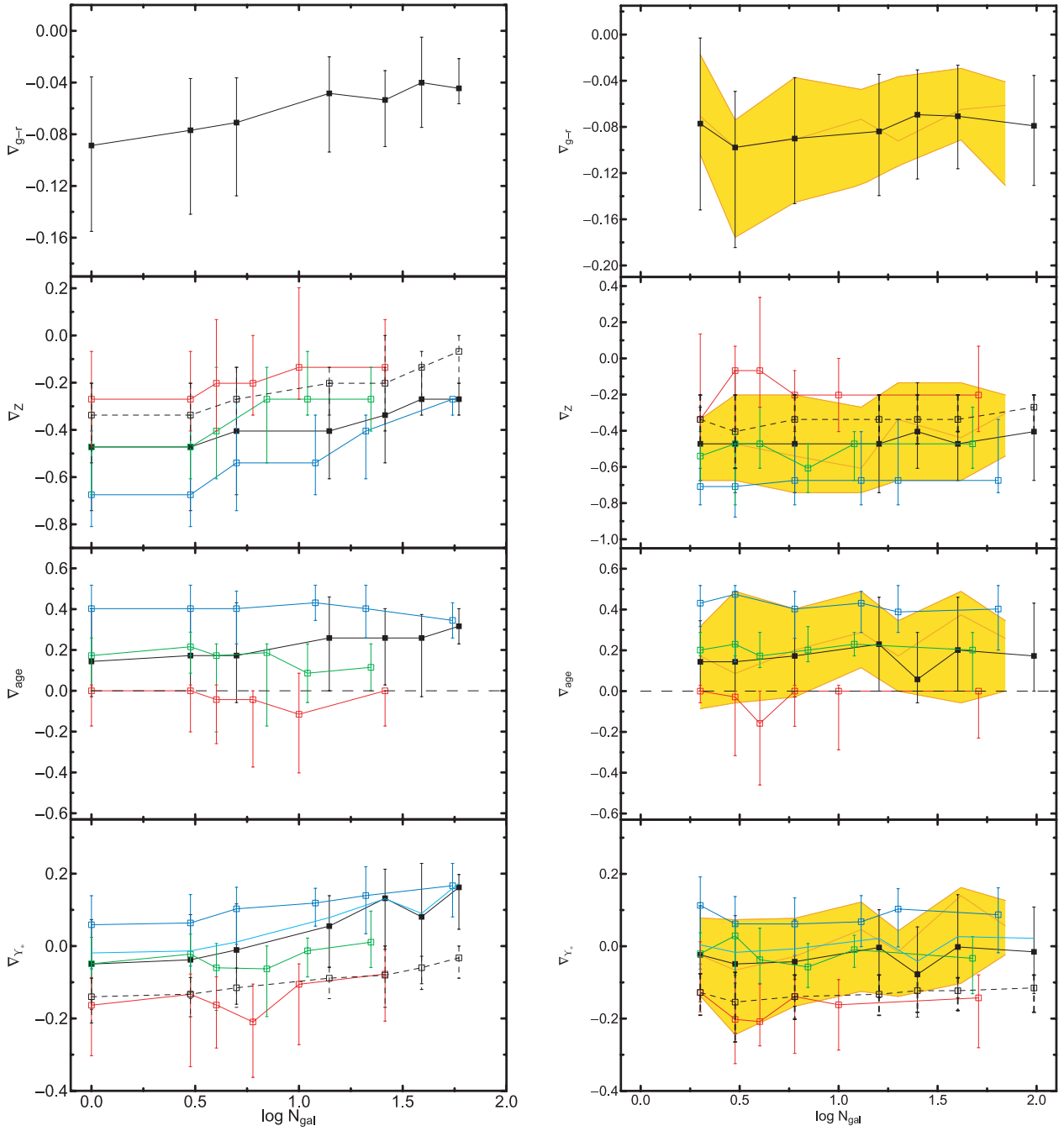

Figure 2. Gradients in terms of the environment for centrals (left) and satellites (right). Medians and 25–75th quantiles are shown. From the top to the bottom, colour, metallicity, age and *M*/*L* gradients are plotted as a function of $N_{\rm gal}$. The black symbols are as in Fig. 1. Moreover, blue, green and red symbols are for galaxies with central age in the intervals $0 < {\rm age}_1 \leq 6$, $6 < {\rm age}_1 \leq 10$ and ${\rm age}_1 > 10$ Gyr, respectively. In the bottom panel, the cyan line is relative to the *V*-band *M*/*L* gradients. Orange lines and yellow regions set medians and 25–75th quantiles for the second most massive galaxy in each group.

As a comparison, we also show in Fig. 2 the results when galaxy colours are fitted to a synthetic spectral model with no age gradient. In this case, metallicity gradients turn out to be shallower, independently of $N_{\rm gal}$, while *M*/*L* gradients are steeper. Note that these last trends are consistent with what was found for the older galaxies in the reference fit. In centrals, the trend is almost unchanged for ∇_Z, while a shallower slope is found for ∇_{Υ_*}. For satellites, slopes resulted unchanged. For completeness, in the bottom panel we also compare with *V*-band *M*/*L* gradients, which despite a slight shift are very similar to the reference *B*-band ones.

We have finally checked that the different trends in Fig. 2 between centrals and satellites survive if we cut the most massive galaxies with $\log M_*/{\rm M}_\odot > 11.4$ or if we include in our sample the galaxies with $10 < \log M_*/{\rm M}_\odot \leq 10.5$.

If we bin the galaxies in terms of stellar mass, we find that if considering the lower mass galaxies the trends in Fig. 2 for centrals

disappear, while for more massive systems the trends become more significant and also the $N_{\rm gal}-{\rm M}_*$ relation is steeper. On the contrary, if we bin the gradients–M_* relations in Fig. 1 in terms of $N_{\rm gal}$, we find that field galaxies show some trends in $\nabla_{\rm age}$ and ∇_Z, which are stronger in group centrals.

4 DISCUSSION AND CONCLUSIONS

In this paper we have investigated the correlation between the colour, *M*/*L* and stellar population gradients with environment for a sample of local central and satellite SDSS central galaxies (B05). We have found some indications which point to a different behaviour in terms of stellar mass and the environment for central and satellite galaxies. Central galaxies dominate the galaxy sample in the massive side, thus have gradients which behave like in T+10 and T+11 when the gradients are plotted in terms of M_*, with ∇_{g-r}, ∇_{Υ_*} and ∇_Z getting shallower and $\nabla_{\rm age}$ (positive) steeper in the most massive galaxies. In contrast, satellite galaxies have a ∇_{g-r} which is less dependent on M_*. Thus, while $\nabla_{\rm age}$ are steeper at larger masses (where they drive the trend of ∇_{Υ_*}), metallicity gradients show a shallower trend. The steeper and stronger trend of ∇_Z and the slightly shallower ∇_Z in the most massive centrals, when compared with satellites, are consistent with the role of dry mergings (Kobayashi 2004), which are more efficient to mix stellar populations at the largest masses where their fraction is larger (i.e. de Lucia et al. 2006). Shallower trends are found in satellites, suggesting a minor role of such kind of phenomena. In satellites, we have found a strong trend of $\nabla_{\rm age}$ with mass (stronger than the one found in centrals), with very massive satellites having steeper $\nabla_{\rm age}$, and thus younger cores. These surviving young cores could be due to bursts of star formation after gas-rich mergers or close encounters. In T+10 we have also seen that central age has an important role, since centrally younger galaxies have steeper gradients, while older systems have, on average, null $\nabla_{\rm age}$ and shallower ∇_Z. This seems consistent with the intervention of processes like dry mergings, which are responsible for a star formation suppression and a mixing of stellar population.[4]

Plotting the gradients in terms of the number of galaxies inside the group, $N_{\rm gal}$, for central galaxies, we find that age gradients seem less dependent on the environment, while colour, *M*/*L* and metallicity gradients are shallower in denser environment (with a number of galaxies in the groups of $N_{\rm gal} \sim 50$ or more) when compared with isolated galaxies. This correlation is even stronger when galaxies are classified in terms of their central ages, which have been shown to drive the scatter of the relation between metallicity/age gradients and mass. On the contrary, massive satellite galaxies do not present any trend with $N_{\rm gal}$ (and independently on the age bin adopted). Consistently with the results found in terms of stellar mass, while dry mergings seem to be important process in massive centrals, no strong indication is found for satellites. Finally, we have also checked that ranking satellites on the basis of their masses, and considering the second most massive galaxy in each group, some slight positive correlations seem to appear in our trends in Fig. 2. These findings suggest that if on the one hand conclusions on centrals are firm and clear, on the other hand satellites results are more complicated to interpret. More detailed analysis would investigate the correlation of population gradients not only with $N_{\rm gal}$, but also with the local and global density, the distance from the centre of the groups and the mass ranking in the group, which all together give a more complete representation of the environmental properties.

The positive correlations found between colour and *Z* gradients with both M_* and $N_{\rm gal}$ in central galaxies are not completely independent each others, since it is easy to show that more massive central galaxies are residing in denser environments with larger cluster/group haloes and populated by a larger number of galaxies (e.g. Stott et al. 2008, 2010; Whiley et al. 2008).

The systematics on the gradients have been investigated in the Appendix A, where we have shown that ∇_{Υ_*} is very little affected (see e.g. T+11), while a shift and a larger scatter could be induced in the estimates of $\nabla_{\rm age}$ and ∇_Z. The trend with M_* and $N_{\rm gal}$ could be possibly affected, in the sense that the true trends for ∇_Z can be shallower or flat and the one for $\nabla_{\rm age}$ steeper (in the worst cases when input data are strongly inaccurate).

From the observational point of view, these are the first steps in the systematic study of the correlations between stellar population gradients and the environment as measured by $N_{\rm gal}$ where the behaviour of the central galaxies is distinguished by the one of satellites (see e.g. La Barbera et al. 2011). Former studies made no selection on the galaxy type (centrals or satellites), and found that colour gradients in massive galaxies are shallower in denser environment (Tamura & Ohta 2000; Ko & Im 2005; La Barbera et al. 2005) similarly to our findings, although La Barbera et al. (2011) have shown that the optical–IR ∇_{g-K} is almost independent of the environment. Along the same line, Roche, Bernardi & Hyde (2010) have demonstrated that central galaxies have shallower gradients than normal E/S0 galaxies at the same luminosity.

For what concerns stellar population gradients, Spolaor et al. (2009) (their right-hand panel in Fig. 1) have compared central galaxies in both clusters and groups with those in the field, but a clear trend is not found since the scatter of the data is too large and the sample too small. Using a combined sample of satellite and central galaxies, La Barbera et al. (2011) have found that $\nabla_{\rm age}$ are slightly increasing with M_* (similarly to our Fig. 1), while ∇_Z decreases, and galaxies in groups present steeper $\nabla_{\rm age}$ and ∇_Z, which are in contrast with our results. The latter discrepant results may be a consequence of a different sample selection or systematics in our stellar population models. In fact, while in our case the number of centrals is dominant, by contrast they adopt a sample without any selection of centrals and satellites, with the latter being dominant. Also in our case, if we would re-do the same plots as in Fig. 2 for the whole sample (i.e. centrals and satellites together), then we would find equally no trend in agreement with La Barbera et al. (2011). Then, if we consider the worst case analysed in simulations discussed in the Appendix A (see e.g. Fig. A1), there seem to be some spurious trends introduced by the use of the optical bands only: if we correct our results for this systematics we can also conclude that a steeper trend with mass for $\nabla_{\rm age}$ and a shallower trend (if any) for ∇_Z would be accommodated by our data, in a way more consistent with La Barbera et al. (2011) findings. If this is the case, it might indicate a major role of gas-rich mergings, cold accretion at high redshift, later gas accretion or close encounters, in satellites, in order to produce steeper gradients in very massive galaxies, rather than dry merging as we would conclude if the gradients are shallower like optical data suggest. Model systematics seem to weakly affect the conclusions with $N_{\rm gal}$ though, which clearly indicates a difference of the gradient behaviour between central galaxies and satellites.

[4] A comment is in order here. Metallicity gradients are less sensitive to recent starburst events, while they are more indicative of the total integrated star formation history. This is because the metal content responds more slowly to the star formation as metals are not strongly altered by new stars, but instead by the integral of all the star formation history. On the other hand, age gradients are by definition sensitive to (significant) starburst events.

Our results give an indication of the role of physical processes in the mass accretion of massive central and satellite galaxies. The effect of merging and, in general, of interactions with environment crucially depends on the kind of process under analysis (minor versus major merging, dry versus wet mergings, accretion, stripping, etc). For example, the positive age gradients found mainly in both (centrally young) central and satellite galaxies support two kinds of processes: (i) a dissipative formation picture, whereby wet mergers fuel the central region with cold gas (de Lucia et al. 2006), or (ii) cold accretion at high redshift (Dekel & Birnboim 2006), which generate the observed younger stellar populations in the centre. But, central galaxies have more chances to merge or interact with neighbours in denser environments; in fact, they are predicted to have larger masses in clusters when compared with similar galaxies in the centres of groups (Romeo et al. 2008). The flatter gradients of centrals we observe in denser environments are consistent with the intervention of a larger number of dry (major) galaxy mergings, which are predicted to mesh stellar populations inside the galaxies (e.g. White 1980; Kobayashi 2004). On the contrary, satellite galaxies do not show any strong evidence in favour of this kind of merging events. The observed younger cores in the youngest galaxies suggest that mergings was not so effective to erase these pre-existing age gradients (possibly generated after a gas-rich merging or cold accretion) or some recent accretion in the centre has happened. While dry mergings were really efficient to dilute those gradients in older galaxies.

The results discussed in this paper represent an useful reference exercise for further analysis performed on higher-z samples, typically involving optical rest frame bandpasses (e.g. from the VLT Survey Telescope, VST). Future analysis with wider wavelength baselines will help to alleviate the problem of parameter degeneracies in stellar modelling (e.g. La Barbera et al. 2011).

ACKNOWLEDGMENTS

CT was supported by the Swiss National Science Foundation.

REFERENCES

Bernstein J. P., Bhavsar S. P., 2001, MNRAS, 322, 625
Blanton M. R. et al., 2005, AJ, 129, 2562 (B05)
Bruzual A. G., Charlot S., 2003, MNRAS, 344, 1000 (BC03)
Chabrier G., 2001, ApJ, 554, 1274
Davis M., Efstathiou G., Frenk C. S., White S. D. M., 1985, ApJ, 292, 371
de Lucia G., Springel V., White S. D. M., Croton D., Kauffmann G., 2006, MNRAS, 366, 499
Dekel A., Birnboim Y., 2006, MNRAS, 368, 2
di Matteo P., Pipino A., Lehnert M. D., Combes F., Semelin B., 2009, A&A, 499, 427
Dressler A., 1978, ApJ, 223, 765
Gallazzi A., Charlot S., Brinchmann J., White S. D. M., Tremonti C. A., 2005, MNRAS, 362, 41
Hopkins P. F., Cox T. J., Dutta S. N., Hernquist L., Kormendy J., Lauer T. R., 2009, ApJS, 181, 135
Jarrett T. H., Chester T., Cutri R., Schneider S. E., Huchra J. P., 2003, AJ, 125, 525
Kawata D., 2001, ApJ, 558, 598
Kawata D., Gibson B. K., 2003, MNRAS, 340, 908
Ko J., Im M., 2005, J. Korean Astron. Soc., 38, 149
Kobayashi C., 2004, MNRAS, 347, 740
Kuntschner H. et al., 2010, MNRAS, 408, 97
La Barbera F., de Carvalho R. R., Gal R. R., Busarello G., Merluzzi P., Capaccioli M., Djorgovski S. G., 2005, ApJ, 626, 19
La Barbera F., Ferreras I., de Carvalho R. R., Lopes P. A. A., Pasquali A., de la Rosa I. G., De Lucia G., 2011, ApJ, 740, 41
Larson R. B., 1974, MNRAS, 166, 585
Larson R. B., 1975, MNRAS, 173, 671
Martin D. C. et al., 2005, ApJ, 619, L1
Mihos J. C., Hernquist L., 1994, ApJ, 437, L47
Pipino A., D'Ercole A., Chiappini C., Matteucci F., 2010, MNRAS, 407, 1347
Rawle T. D., Smith R. J., Lucey J. R., 2010, MNRAS, 401, 852
Roche N., Bernardi M., Hyde J., 2010, MNRAS, 407, 1231
Romeo A. D., Napolitano N. R., Covone G., Sommer-Larsen J., Antonuccio-Delogu V., Capaccioli M., 2008, MNRAS, 389, 13
Schombert J. M., 1986, ApJS, 60, 603
Sijacki D., Springel V., Di Matteo T., Hernquist L., 2007, MNRAS, 380, 877
Spolaor M., Proctor R. N., Forbes D. A., Couch W. J., 2009, ApJ, 691, 138
Spolaor M., Kobayashi C., Forbes D. A., Couch W. J., Hau G. K. T., 2010, MNRAS, 408, 272
Springel V. et al., 2005, Nat, 435, 629
Stott J. P., Edge A. C., Smith G. P., Swinbank A. M., Ebeling H., 2008, MNRAS, 384, 1502
Stott J. P. et al., 2010, ApJ, 718, 23
Tamura N., Ohta K., 2000, AJ, 120, 533
Tortora C., Napolitano N. R., Cardone V. F., Capaccioli M., Jetzer Ph., Mdinaro R., 2010, MNRAS, 407, 144 (T+10)
Tortora C., Romeo A. D., Napolitano N. R., Antonuccio-Delogu V., Meza A., Sommer-Larsen J., Capaccioli M., 2011a, MNRAS, 411, 627
Tortora C., Napolitano N. R., Romanowsky A. J., Jetzer Ph., Cardone V. F., Capaccioli M., 2011b, MNRAS, 418, 1557
Weinmann S. M., Kauffmann G., van den Bosch F. C., Pasquali A., McIntosh D. H., Mo H., Yang X., Guo Y., 2009, MNRAS, 394, 1213
Whiley I. M. et al., 2008, MNRAS, 387, 1253
White S. D. M., 1980, MNRAS, 191, 1
Worthey G., 1994, ApJS, 95, 107
Yang X., Mo H. J., van den Bosch F. C., Pasquali A., Li C., Barden M., 2007, ApJ, 671, 153

APPENDIX A: SYSTEMATICS IN THE STELLAR FIT

Here, we check for systematic effects on our gradient ($\nabla_{\rm age}$ and ∇_Z) estimates from the stellar population fits. Because of the well-known age–metallicity degeneracy (Worthey 1994; Bruzual & Charlot 2003; Gallazzi et al. 2005), the stellar population parameters and the gradients might be biased when using the optical colours only, as we do now. Widening the wavelength baseline to include near-infrared (NIR) colours should ameliorate the degeneracy. Although the synthetic prescriptions in the NIR region of the spectra are still uncertain, it is very important to understand their impact on our analysis. In T+10 and T+11, we checked age and metallicity inferences using optical versus optical+NIR constraints, and found, on average, little systematic difference. Anyway, depending case by case, a spurious shift can appear in the estimated gradients and a wide scatter when the fit is made only using optical data. Here we will carry out a similar analysis to study the trends with stellar mass and $N_{\rm gal}$, using a suite of Monte Carlo simulations. Because of the large amount of details involved, we will consider the results from these simulations as a qualitative guide to understand in what direction the correlations found would change.

We extract 1000 simulated galaxy spectra from our BC03 spectral energy distribution libraries with random, uncorrelated stellar parameters and gradients. In order to have gradients similar to the ones we observe, we only impose some constraints on the input stellar parameters, producing, on average, $\nabla_{\rm age} \sim 0.2$ and $\nabla_Z \sim -0.3$. We add simulated (equal) measurement errors for each

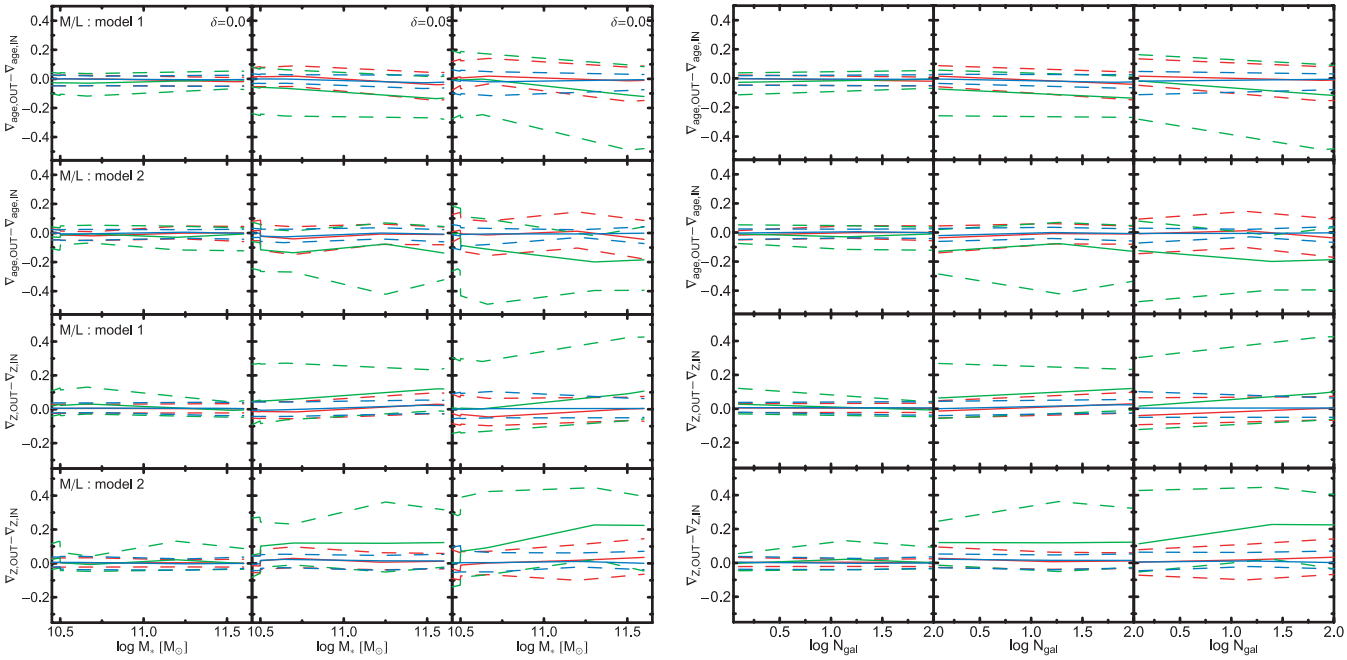

Figure A1. Systematics in stellar population fitting in terms of stellar mass (left-hand panels) and galaxy number in the groups (right-hand panels). We define the quantity $\nabla_{X,\rm OUT} - \nabla_{X,\rm IN}$, where $X = $ (age, Z), IN and OUT are the input and output values. In each big panel, from the top to the bottom we show the systematics in age gradients for two M/L–M_* relations and Z gradients for the same two M/L–M_* relations. From the left to the right, we show the cases $\delta = 0.01$, 0.03 and 0.05. The continuous line is the median while dashed ones are the 25–75th quantiles. Green, red and blue are for the fit using optical, optical+NIR and optical+UV, respectively.

band, as randomly extracted steps from the interval $(-\delta, +\delta)$, with $\delta = 0.01, 0.03, 0.05$. We apply our fitting procedure and then compare the output parameter estimates to the input model values. We perform the fit (1) using only the optical SDSS bands *ugriz* and (2) adding NIR photometry (J, H and $K_{\rm s}$; Jarrett et al. 2003) and (3) UV photometry (near-UV and far-UV; Martin et al. 2005). Finally, to plot the results in terms of stellar mass we have adopted two linear relation to convert the M/L values into stellar mass. As test relations we have recovered from our results at R_1 and R_2 the following best relations: $\log M/L = -0.75 + 0.11 \log {\rm M}_*$ and $\log M/L = -1.08 + 0.15 \log {\rm M}_*$. Moreover, the best-fitting relation between stellar mass and $N_{\rm gal}$ have been derived and used to plot the shift in the gradients in term of $N_{\rm gal}$.

We define the quantity $\nabla_{X,\rm OUT} - \nabla_{X,\rm IN}$, where $X = $ (age, Z), IN and OUT are the input and output X values. In Fig. A1 we show the $\nabla_{X,\rm OUT} - \nabla_{X,\rm IN}$ as a function of M_* and $N_{\rm gal}$, for both age and metallicity and the two M/L–M_* relations. We find that, adding the NIR or UV data, the gradients, independently from the shift δ adopted, are perfectly recovered with a very little scatter. With optical data only, the uncertainties are larger and some systematic shifts emerge, mainly for $\delta \geq 0.03$. In this case, our predicted $\nabla_{\rm age}$ and ∇_Z are underestimated and overestimated with respect to the input values, respectively. These discrepancies are larger for galaxies with larger M_* and $N_{\rm gal}$, and in the worst case can amount to $\sim$0.1 with respect to the ones with lower M_* and $N_{\rm gal}$, for $\delta = 0.05$. Although these findings would led to a possible flattening of the trends of ∇_Z in terms of mass and $N_{\rm gal}$, a weaker trend would survive. If one assumes a constant relation between stellar mass and $N_{\rm gal}$, as for satellites, the trend with $N_{\rm gal}$ in Fig. A1 would be cancelled and a simple offset in gradient trends would arise in Fig. 2.

This paper has been typeset from a TEX/LATEX file prepared by the author.